STUDY OF CONTINUOUS SPILL WITH A LIMITED PERIOD OF RELEASE

Kim, M.[1], Do, K.[2], Kim, T.[3], Choi, B.[4] and Han, Y.[5]

[1] Division of Energy Plant Safety, Korea Institute of Machinery & Materials, Gajeongbukno 156, Yusong, Daejeon, 305-343, South Korea, mbkim@kimm.re.kr

[2] Division of Energy Plant Safety, Korea Institute of Machinery & Materials, Gajeongbukno 156, Yusong, Daejeon, 305-343, South Korea, kyudo@kimm.re.kr

[3] Division of Energy Plant Safety, Korea Institute of Machinery & Materials, Gajeongbukno 156, Yusong, Daejeon, 305-343, South Korea, taehoon@kimm.re.kr

[4] Division of Energy Plant Safety, Korea Institute of Machinery & Materials, Gajeongbukno 156, Yusong, Daejeon, 305-343, South Korea, cbisey@kimm.re.kr

[5] Division of Energy Plant Safety, Korea Institute of Machinery & Materials, Gajeongbukno 156, Yusong, Daejeon, 305-343, South Korea, yshan@kimm.re.kr

ABSTRACT

In this study, the spread of cryogenic liquid due to a limited period of release is investigated for the first time. This physical phenomenon is governed by three parameters: the evaporation rate per unit area, release time, and spill quantity. However, it is found that two dimensionless parameters, the dimensionless evaporation rate and the dimensionless spill rate, are determined by non-dimensionalizing the governing equation of this phenomenon. Third-order perturbation solutions are obtained and compared with a numerical solution to verify the perturbation solution. For the same spill quantity, continuous and subsequent instantaneous models are necessary for small release times, whereas continuous models are only required for large release times. Additionally, two consecutive spread models are necessary for a small spill quantity at a fixed release time. These two spread regimes are clearly distinguished using the perturbation solution.

1.0 INTRODUCTION

Because the release of flammable materials in a petro-chemical plant likely leads to a fire or an explosion, a study of the release and spread of such materials is essential for the quantitative risk assessment and risk-based inspection of these plants. The release of materials can be classified into vapor phase or liquid phase according to the phase of the material, and the spread of a released liquid is more complicated than that of released gas because evaporation occurs during the spread of a liquid. The present work focuses on the release and spread of a cryogenic liquid, such as LH_2, which is continued work from the previous results[1-2] of authors.

Release can be defined as a loss of containment[3] within components or equipment of several plants; therefore, release means that some materials contained in the equipment escape and spread into atmosphere. Spurted liquids can spread via vaporization from the ground or water, and various models have been developed to treat the spread. There are three-dimensional models using the full Navier-Stokes equation[4], a shallow-layer model[5-9], and a simple physical model[1,2,10]. The shallow-layer model consists of partial differential equations to solve the velocity and pool height with respect to the radius and time under the assumption of axisymmetry. The simplest mathematical model, which can be called a simple physical model, describes pool spread in terms of how the pool radius and height evolve in time. The corresponding equations consist of two ordinary differential equations with respect to time and one algebraic equation. Vaporization can be modeled based on thermal energy conservation or heat conduction from the surface on which the liquid expands and by neglecting heat radiation; however, the concept of constant evaporation rate per unit area has been used to simplify the evaporation process in most cases.

The aforementioned differential equations used in the spread model require initial conditions that depend on the type of release. Release is generally categorized into instantaneous and continuous release. According to API RP 581[3], instantaneous release occurs so rapidly that the fluid disperses as a single cloud or pool, whereas continuous release occurs over a longer period of time. Therefore, it can be said that instantaneous release occurs due to an abrupt destruction of vessels or a similar situation. The case where fluid flows continuously from a small hole in damaged equipment can be modeled as continuous release. Mathematically, in the spread model of instantaneous release, parameters regarding the initial shape of the released liquid are given when time is zero; however, all the parameters are zero at that time in the case of continuous release.

The spread model of continuously- released- fluid can require a period of release time that is not necessary in the spread model of an instantaneously- released- fluid. If the release time is less than the entire time domain, the instantaneous release model should be added to the continuous model from the end of the release time. This combined release that consists of the initial continuous model and subsequent instantaneous model is more realistic. In the present work third-order perturbation solutions are obtained for the first time with the spread of the combined release, and the solutions are compared with numerical solutions that are believed to be exact solutions. Parameters that distinguish continuous release and combined release are discovered and formulated using analytical features of the perturbation solutions.

2.0 GOVERNING EQUATIONS

There are several forces during the spread of liquid. Gravity is only important for the spread of cryogenic liquid because cryogenic liquid vaporizes extremely quickly. If the shape of the spreading liquid is assumed to be a circular cylinder, the governing equations can be obtained with a slight modification of the previous work[2] of the authors.

$$\frac{dR}{dT} = \sqrt{\alpha H}\ , \tag{1}$$

where R - pool radius, m; T – time, s; α - 2gΔ, m/s^2; g - gravity, m/s^2; Δ - 1 for spills on the ground or 1-ρ/ρ_w for spills on water; ρ - density of liquid, kg/m^3; ρ_w - density of water, kg/m^3; H – pool height, m.

$$\frac{dV}{dT} = -E\pi R^2 + \beta; \quad \beta = \frac{Q}{T_d} \quad for \quad 0 \le T \le T_d\,, \quad \beta = 0 \quad for \quad T > T_d\,, \tag{2}$$

where V - pool volume, m^3; E - evaporation rate per unit area, m/s; β - spill source rate, m^3/s; Q – spill volume, m^3; T_d –period of release time, s. To complete the model, the following algebraic equation is required:

$$H = \frac{V}{\pi R^2} \tag{3}$$

If the liquid is continuously released from storage, the following initial conditions can be used:

$$V(0) = 0, \quad R(0) = 0, \quad H(0) = 0 \tag{4}$$

From Equations (1) through (4), it is understood that the evaporation rate per unit area, E, the spill volume, Q, and the period of release time, T_d, govern the model equations for spread on the ground. For simplicity, spread on the ground is considered in the present study. To make the governing equations dimensionless, the following variables are introduced:

$$v = \frac{V}{\pi L^3}, \quad r = \frac{R}{L}, \quad h = \frac{H}{L}, \quad t = \frac{T}{\tau}, \tag{5}$$

where v - dimensionless volume; r - dimensionless radius; h - dimensionless height; t - dimensionless time; τ and L are the characteristic time and length scale defined as

$$\tau = T_d, \quad L = \alpha T_d^2 \tag{6}$$

Using the dimensionless variables in Equation (5), the following non-dimensional governing equations are derived:

$$\frac{dv}{dt} = \beta_* - \varepsilon r^2 : \quad \beta_* = \frac{Q}{\pi \alpha^3 T_d^6} \quad for \quad 0 \le t \le 1, \quad \beta_* = 0 \quad for \quad t > 1, \tag{7}$$

where ε - dimensionless evaporation rate, $E/\alpha T_d$.

$$\frac{dr}{dt} = \sqrt{h} \tag{8}$$

$$h = \frac{v}{r^2} \tag{9}$$

The initial conditions become

$$v(0) = 0, \quad r(0) = 0, \quad h(0) = 0 \tag{10}$$

From Equations (7) through (10), it can be seen that the dimensionless number, ε, corresponding to the dimensionless evaporation rate and the dimensionless spill source rate, β_*, are the parameters that can control the non-dimensional governing equations.

3. PERTURBATION SOLUTIONS

The evaporation rate per unit area of LH_2 on a paraffin wax ground[7] varies from approximately 4.23×10^{-4} m/s to approximately 12.7×10^{-4} m/s. Therefore, the dimensionless evaporation rate, ε, can be naturally chosen as the perturbation parameter. The perturbation solutions can then be expressed in the following forms:

$$v = v_0 + \varepsilon v_1 + \varepsilon^2 v_2 + \varepsilon^3 v_3, \tag{11}$$

where v_0 - zeroth order term, v_1 – 1st order term, v_2 – 2nd order term, v_3 – 3rd order term.

$$r = r_0 + \varepsilon r_1 + \varepsilon^2 r_2 + \varepsilon^3 r_3, \tag{12}$$

where r_0 - zeroth order term, r_1 – 1st order term, r_2 – 2nd order term, r_3 – 3rd order term.

$$h = h_0 + \varepsilon h_1 + \varepsilon^2 h_2 + \varepsilon^3 h_3, \tag{13}$$

where h_0 - zeroth order term, h_1 – 1st order term, h_2 – 2nd order term, h_3 – 3rd order term.

Terms higher than $O(\varepsilon^3)$ are omitted. In this study, a third-order expansion is used, and terms up to $O(\varepsilon^3)$ are retained. Substituting Equations (11) through (13) into Equations (7) through (9) and equating the coefficients of ε^0, ε, ε^2 and ε^3 on both sides, we obtain

$$\frac{dr_0}{dt} = \sqrt{h_0} \tag{14}$$

$$\frac{dr_1}{dt} = \frac{h_1}{2\sqrt{h_0}} \tag{15}$$

$$\frac{dr_2}{dt} = \frac{h_2}{2\sqrt{h_0}} - \frac{h_1^2}{8h_0^{3/2}} \tag{16}$$

$$\frac{dr_3}{dt} = \frac{h_3}{2\sqrt{h_0}} - \frac{h_1}{4h_0^{3/2}}\left(h_2 - \frac{h_1^2}{4h_0}\right) \tag{17}$$

$$\frac{dv_0}{dt} = \beta_*; \quad \beta_* = \frac{Q}{\pi\alpha^3 T_d^6} \quad for \quad 0 \le t \le 1, \quad \beta_* = 0 \quad for \quad t > 1 \tag{18}$$

$$\frac{dv_1}{dt} = -r_0^2 \tag{19}$$

$$\frac{dv_2}{dt} = -2r_0\, r_1 \tag{20}$$

$$\frac{dv_3}{dt} = -r_1^2 - 2r_0\, r_2 \tag{21}$$

$$h_0 = \frac{v_0}{r_0^2} \tag{22}$$

$$h_1 = \frac{v_1}{r_0^2} - \frac{2h_0 r_1}{r_0} \tag{23}$$

$$h_2 = \frac{v_2}{r_0^2} - h_0\left[\frac{2r_2}{r_0} + \left(\frac{r_1}{r_0}\right)^2\right] - \frac{2h_1 r_1}{r_0} \tag{24}$$

$$h_3 = \frac{v_3}{r_0^2} - 2h_0\left[\frac{r_3}{r_0} + \frac{r_1 r_2}{r_0^2}\right] - h_1\left[\frac{2r_2}{r_0} + \left(\frac{r_1}{r_0}\right)^2\right] - \frac{2h_2 r_1}{r_0} \tag{25}$$

Compared with the corresponding equations in the authors' previous work[2], it is noteworthy that Equations (16), (17), (23), (24), and (25) are improved in the present work.

3.1 Continuous Regime ($0 \le t \le 1$)

Twelve new equations (Equations (14) through (25)) have been obtained; therefore, the number of initial conditions must increase to twelve. Applying the conditions in Equation (10) to Equations (11) through (13) and equating the coefficients of ε^0, ε, etc., on both sides, we get

$$v_0(0) = 0, \quad r_0(0) = 0, \quad h_0(0) = 0 \tag{26}$$

$$v_1(0)=0, \quad r_1(0)=0, \quad h_1(0)=0 \tag{27}$$

$$v_2(0)=0, \quad r_2(0)=0, \quad h_2(0)=0 \tag{28}$$

$$v_3(0)=0, \quad r_3(0)=0, \quad h_3(0)=0 \tag{29}$$

Solving Equations (14) through (25) with the initial conditions in Equations (26) through (29) yields

$$r_0 = \frac{2}{\sqrt{3}}\beta_*^{1/4}t^{3/4} \tag{30}$$

$$r_1 = -\frac{2\sqrt{3}}{45}\beta_*^{-1/4}t^{9/4} \tag{31}$$

$$r_2 = -\frac{2\sqrt{3}}{675}\beta_*^{-3/4}t^{15/4} \tag{32}$$

$$r_3 = -\frac{2\sqrt{3}}{4455}\beta_*^{-5/4}t^{21/4} \tag{33}$$

and

$$v_0 = \beta_* t \tag{34}$$

$$v_1 = -\frac{8}{15}\beta_*^{1/2}t^{5/2} \tag{35}$$

$$v_2 = \frac{2}{45}t^4 \tag{36}$$

$$v_3 = \frac{8}{7425}\beta_*^{-1/2}t^{11/2} \tag{37}$$

$$h_0 = \frac{3}{4}\beta_*^{1/2}t^{1/2} \tag{38}$$

$$h_1 = -\frac{3}{10}t \tag{39}$$

$$h_2 = -\frac{1}{300}\beta_*^{-1/2}t^{5/2} \tag{40}$$

$$h_3 = -\frac{1}{2475}\beta_*^{-1}t^4 \tag{41}$$

3.2 Instantaneous Regime ($t \geq 1$)

The solutions in this regime can be obtained using $v(1)$, $r(1)$, and $h(1)$ as initial conditions because the release ends at t=1. From the solutions, we can obtain

$$v_\tau \equiv v(1) = \beta_* - \frac{8}{15}\beta_*^{1/2}\varepsilon + \frac{2}{45}\varepsilon^2 + \frac{8}{7425}\beta_*^{-1/2}\varepsilon^3 \tag{42}$$

$$r_\tau \equiv r(1) = \frac{2}{\sqrt{3}}\beta_*^{1/4} - \frac{2\sqrt{3}}{45}\beta_*^{-1/4}\varepsilon - \frac{2\sqrt{3}}{675}\beta_*^{-3/4}\varepsilon^2 - \frac{2\sqrt{3}}{4455}\beta_*^{-5/4}\varepsilon^3 \tag{43}$$

$$h_\tau \equiv h(1) = \frac{3}{4}\beta_*^{1/2} - \frac{3}{10}\varepsilon - \frac{1}{300}\beta_*^{-1/2}\varepsilon^2 - \frac{1}{2475}\beta_*^{-1}\varepsilon^3 \tag{44}$$

A new time coordinate is introduced for convenience as follows:

$$t' = t - 1 \tag{45}$$

For the initial conditions for the continuous regime, the following initial conditions in view of the new time are obtained:

$$v_0(t'=0) = v_\tau, \quad r_0(t'=0) = r_\tau, \quad h_0(t'=0) = h_\tau \tag{46}$$

$$v_1(t'=0) = 0, \quad r_1(t'=0) = 0, \quad h_1(t'=0) = 0 \tag{47}$$

$$v_2(t'=0) = 0, \quad r_2(t'=0) = 0, \quad h_2(t'=0) = 0 \tag{48}$$

$$v_3(t'=0) = 0, \quad r_3(t'=0) = 0, \quad h_3(t'=0) = 0 \tag{49}$$

Solving Equations (14) through (25) with the initial conditions in Equation (46) through (49) yields

$$r_0 = \sqrt{r_\tau^2 + 2v_\tau^{1/2}t'} \tag{50}$$

$$v_0 = v_\tau \tag{51}$$

$$h_0 = \frac{v_\tau}{r_\tau^2 + 2v_\tau^{1/2}t'} \tag{52}$$

$$r_1 = -\frac{1}{2\sqrt{v_\tau(r_\tau^2 + 2v_\tau^{1/2}t')}}\left(\frac{v_\tau^{1/2}t'^3}{3} + \frac{r_\tau^2 t'^2}{2}\right) \tag{53}$$

$$v_1 = -v_\tau^{1/2}t'^2 - r_\tau^2 t' \tag{54}$$

$$h_1 = -\frac{v_\tau^{1/2}t'^2 + r_\tau^2 t'}{r_\tau^2 + 2v_\tau^{1/2}t'} + \frac{v_\tau^{1/2}}{\left(r_\tau^2 + 2v_\tau^{1/2}t'\right)^2}\left(\frac{v_\tau^{1/2}t'^3}{3} + \frac{r_\tau^2 t'^2}{2}\right) \tag{55}$$

$$r_2 = -\frac{1}{v_\tau^4(r_\tau^2 + 2v_\tau^{1/2}t')^{3/2}}\left(\frac{17}{360}v_\tau^4 t'^6 + \frac{17}{120}v_\tau^{7/2}r_\tau^2 t'^5 + \frac{5}{32}v_\tau^3 r_\tau^4 t'^4 + \frac{1}{24}v_\tau^{5/2}r_\tau^6 t'^3\right) \tag{56}$$

$$v_2 = \frac{1}{12}t'^4 + \frac{1}{6}v_\tau^{-1/2}r_\tau^2 t'^3 \tag{57}$$

$$h_2 = -\frac{1}{(r_\tau^2 + 2v_\tau^{1/2}t')^3}\left(\frac{7}{45}v_\tau t'^6 + \frac{7}{15}v_\tau^{1/2}r_\tau^2 t'^5 + \frac{7}{12}r_\tau^4 t'^4 + \frac{1}{4}v_\tau^{-1/2}r_\tau^6 t'^3\right) \tag{58}$$

$$r_3 = -\frac{1}{(r_\tau^2 + 2v_\tau^{1/2}t')^{5/2}}\left(\begin{array}{l}\frac{13}{432}t'^9 + \frac{13}{96}v_\tau^{-1/2}r_\tau^2 t'^8 + \frac{81}{320}v_\tau^{-1}r_\tau^4 t'^7 + \frac{1361}{5760}v_\tau^{-3/2}r_\tau^6 t'^6 + \frac{1}{10}v_\tau^{-2}r_\tau^8 t'^5 + \\ \frac{1}{64}v_\tau^{-5/2}r_\tau^{10}t'^4\end{array}\right) \tag{59}$$

$$v_3 = \frac{1}{180}v_\tau^{-1/2}t'^6 + \frac{1}{60}v_\tau^{-1}r_\tau^2 t'^5 + \frac{1}{48}v_\tau^{-3/2}r_\tau^4 t'^4 \tag{60}$$

$$h_3 = -\frac{1}{(r_\tau^2 + 2v_\tau^{1/2}t')^4}\left(\begin{array}{l}\frac{2}{27}v_\tau t'^9 + \frac{1}{3}v_\tau^{1/2}r_\tau^2 t'^8 + \frac{113}{180}r_\tau^4 t'^7 + \frac{217}{360}v_\tau^{-1/2}r_\tau^6 t'^6 + \frac{21}{80}v_\tau^{-1}r_\tau^8 t'^5 + \\ \frac{1}{32}v_\tau^{-3/2}r_\tau^{10}t'^4\end{array}\right) \tag{61}$$

4. RESULTS AND DISCUSSION

To evaluate the perturbation solutions, numerical solutions based on the Runge-Kutta method are accurately obtained after several trials. Under the assumption that the numerical solutions have adequate accuracy, these solutions are used to verify the perturbation solutions. For the purpose of numerical evaluation, a spreading of LH_2 on the ground with E =4.2×10^{-4} m/s was considered.

The third-order perturbation solutions and the numerical solutions are calculated for release times of 0.1 s, 1 s, and 30 s with a fixed spill volume of 1 m^3 to explore the effect of the release time on the solutions. In the case of the pool volume, two types of solutions for small times of release (T_d=0.1, 1 s) are indistinguishable over the entire period of time, as seen in Figs. 1-2; however, there is a small difference between the two solutions in the late stage of spread, shown in Fig. 3. These characteristics of the perturbation solutions are well known, even in the previous work[2]. A similar tendency can be seen for the pool radius in Figs. 4-6, except for the small difference between two solutions over the late stage of spread despite the small time of release.

The third-order perturbation solutions are illustrated with a fixed spill volume of 1 m^3 in Fig. 7 to understand the effect of the release time on the spread pattern in detail. Discontinuous points are found in the curves of the pool volume with time when the release time is less than or equal to 20 s. These points are boundaries between the initial continuous releases and the following instantaneous releases. In other words, the points represent the end of the continuous releases and simultaneously, the beginning of the instantaneous releases. As the release time increases to 30 s, the discontinuous point disappears because only the continuous mode exists in the spread. It is notable that the pool volume becomes zero before the release is stopped in this case because if the spill source rate, the ratio of the spill volume to the release time, is small, the evaporation from the pool is larger than the supply to the pool, as described by Equation (2). Therefore, logically, the transition to the opposite direction will lead to the pure instantaneous mode. When the release time is infinitesimally small, the pure instantaneous mode will be obtained.

To see the other tendency, the effect of the spill volume on the spread pattern with fixed a released time of 30 s was studied. A similar spread pattern can be seen in Fig. 8, where there are also discontinuous points in the combined released mode with Q=10 and 100 m^3, and the pure continuous mode in the case of a small released volume with Q=0.1 m^3 is shown in Fig. 7. Therefore, the pure continuous mode can be defined as the spread in which evaporation is completed within the release time. The boundary between the continuous mode and the combined mode is determined by following condition:

$$v(t=1)=0 \tag{62}$$

Applying the above equation to the solution of the continuous mode, Equations (34) through (37), we obtain

$$\beta_* - \frac{8}{15}\beta_*^{1/2}\varepsilon + \frac{2}{45}\varepsilon^2 + \frac{8}{7425}\beta_*^{-1/2}\varepsilon^3 = 0 \tag{63}$$

Solving Equation (63) gives

$$\varepsilon = 2.370\sqrt{\beta_*} \tag{64}$$

In the case of second-order solutions, the coefficient in Equation (64) changes to 2.326. Substituting the corresponding dimensional quantities into Equation (64), we finally obtain

$$T_d^2 = 2.370\frac{1}{E}\sqrt{\frac{Q}{\pi\alpha}} \tag{65}$$

Fig. 9 shows a diagram that can show two regimes regarding the release mode.

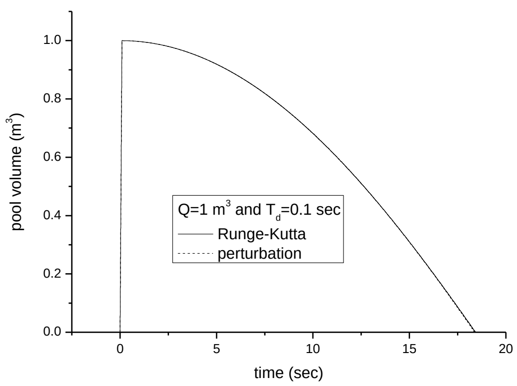

Figure 1. Pool volume vs. time with T_d=0.1 s.

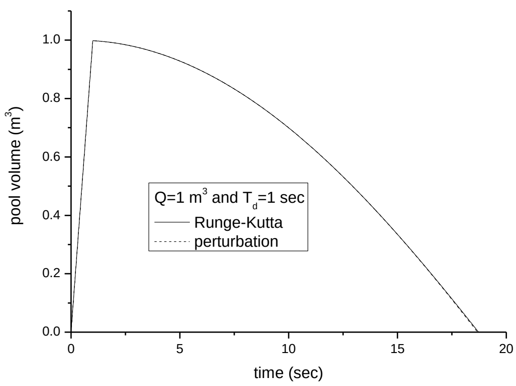

Figure 2. Pool volume vs. time with T_d=1 s.

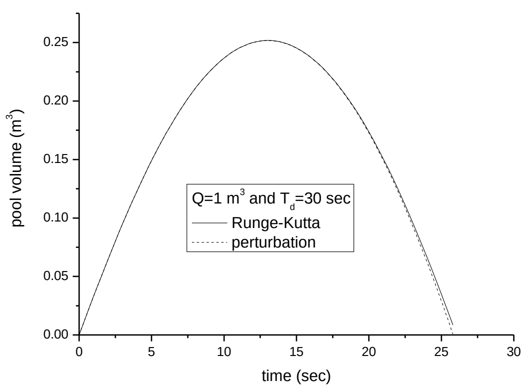

Figure 3. Pool volume vs. time with T_d=30 s.

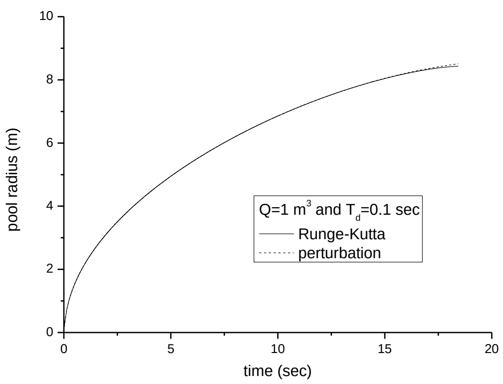

Figure 4. Pool radius vs. time with T_d=0.1 s.

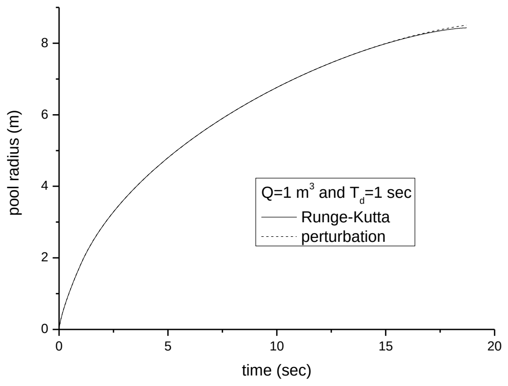

Figure 5. Pool radius vs. time with T_d=1 s.

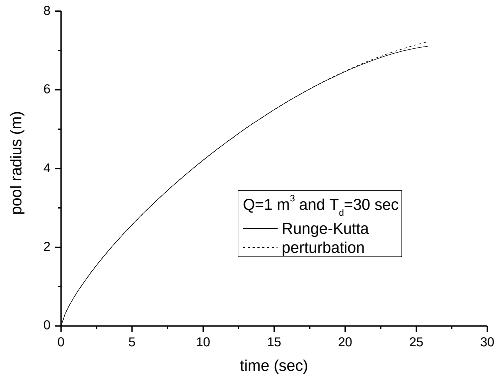

Figure 6. Pool radius vs. time with T_d=30 s.

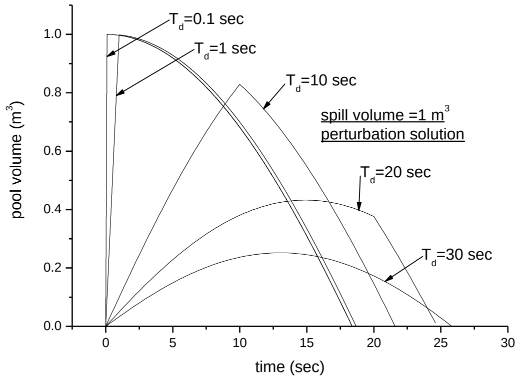

Figure 7. Pool spread pattern with release time

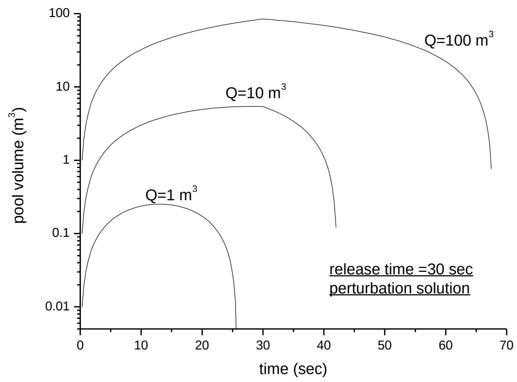

Figure 8. Pool spread pattern with spill volume

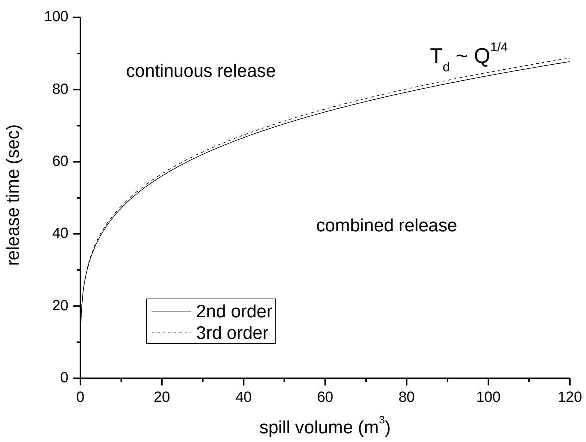

Figure 9. Classification of the release mode

5. CONCLUSIONS

When cryogenic liquids, such as LH_2 or LNG, leak from plant equipment, the concepts of continuous and instantaneous release are used. For the consequence analysis in API RBI assessment[3], two types of release are also defined. The release models decide part of the governing equations and an initial condition. Liquids leak continuously until the released liquids vaporize completely in the continuous release model, whereas the instantaneous model handles only instantaneously- released- liquid. Therefore, the release and the spread are simultaneously maintained until complete vaporization in continuous mode is achieved; however, in instantaneous mode, the spread is only considered because the release occurs instantaneously.

For the present work, the spread due to the continuous release with a limited release time is treated. The spread due to this type of release becomes the combined release that consists of the initial continuous mode and the following instantaneous mode. The subsequent instantaneous mode begins from the time when the leak stops. It is discovered that the model equations for the spread on the ground is governed by three parameters: the evaporation rate per unit area, the spill volume, and the release time. To obtain more general solutions, non-dimensional governing equations are deduced based on characteristic scales. It is revealed that the dimensionless evaporation rate and the dimensionless spill source rate are the parameters that can control the non-dimensional governing equations. It is noteworthy that the governing parameters diminish from three to two through the non-dimensionalization of the governing equations.

The third-order perturbation solutions are obtained and agree well with the numerical solutions for the dimensionless governing equations. It is discovered that both the combined release mode and the pure continuous mode can exist via the relationship of the evaporation rate per unit area, the release time, and the spill volume. Under the assumption of constant evaporation rate per unit area, the realm of the two release modes is distinguished in the coordinate system of the release time and the spill volume using the analytical feature of the perturbation solution. It should be noted that the concept of the three modes of release are established more scientifically, which is different from the conventional concept, such as API RBI 581[3].

ACKNOWLEDGEMENT

This research was supported by the Converging Research Center Program funded by the Ministry of Education, Science and Technology of Korea (Grant number: 2012K001437).

REFERENCES

1. Kim, M., Do, K., Choi, B. and Han, Y., First-order perturbation solutions of liquid pool spreading with vaporization, *Int J Hydrogen Energy,* **36**, 2011, pp.3268-3271.
2. Kim, M., Do, K., Choi, B. and Han, Y., High-order perturbation solutions to a LH_2 spreading model with continuous spill, *Int J Hydrogen Energy*, **37**,2012, pp.17409-17414.
3. API RP 581 PART 3, Consequence analysis in an API RBI assessment, American Petroleum Institute, Washington, D. C., 2008, p.8.
4. Venetsanos, A. G. and Bartzis, J. G., CFD modeling of large-scale LH2 spills in open environment, Proceedings of the First International Conference on Hydrogen Safety, Pisa, Italy, 2005, pp.125-136.
5. Stein, W. and Ermak, D. L., One-dimensional numerical fluid dynamics model of the spreading of liquefied gaseous fuel(LGF) on water, Lawrence Livermore National Laboratory Report No. UCRL-53078, 1980.
6. Verfondern, K. and Dienhart, B., Experimental and theoretical investigation of liquid hydrogen pool spreading and vaporization, *Int J Hydrogen Energy*, **22**, No. 7, 1997, pp.649-660.

7. Verfondern, K. and Dienhart, B., Pool spreading and vaporization of liquid hydrogen, *Int J Hydrogen Energy*, **32**, 2007, pp.256-267.
8. Brandeis, J. and Kansa, E., Numerical simulation of liquefied fuel spills: I. Instantaneous release into a confined area, *Int J Numer Methods Fluids,* **3**, 1983, pp.333-345.
9. Brandeis, J. and Ermak, D., Numerical simulation of liquefied fuel spills: II. Instantaneous and continuous LNG spills on an unconfined water surface. *Int J Numer Methods Fluids*, **3**, 1983, pp. 347-361.
10. Briscoe, F. and Shaw, P., Spread and evaporation of liquid. *Progr Energy Comb Sci*, **6,** 1980, pp. 127-140.